Dynamical Coulomb Blockade of Shot Noise

Carles Altimiras, Olivier Parlavecchio, Philippe Joyez, Denis Vion, Patrice Roche, Daniel Esteve, Fabien Portier

HAL Id: cea-01384659

https://hal-cea.archives-ouvertes.fr/cea-01384659

Submitted on 20 Oct 2016

Dynamical Coulomb Blockade of Shot Noise

Carles Altimiras,* Olivier Parlavecchio, Philippe Joyez, Denis Vion, Patrice Roche, Daniel Esteve, and Fabien Portier[†]

Service de Physique de l'Etat Condensé (CNRS URA 2464),
IRAMIS, CEA-Saclay, 91191 Gif-sur-Yvette, France
(Dated: September 5, 2013)

We observe the suppression of the finite frequency shot-noise produced by a voltage biased tunnel junction due to its interaction with a single electromagnetic mode of high impedance. The tunnel junction is embedded in a $\lambda/4$ resonator containing a dense SQUID array providing it with a characteristic impedance in the kΩ range and a resonant frequency tunable in the 4-6 GHz range. Such high impedance gives rise to a sizeable Coulomb blockade on the tunnel junction ($\sim$30% reduction in the differential conductance) and allows an efficient measurement of the spectral density of the current fluctuations at the resonator frequency. The observed blockade of shot-noise is found in agreement with an extension of the dynamical Coulomb blockade theory.

Contrarily to usual electronic components for which one can define an intrinsic behavior (e.g. the I-V characteristic), the transport properties of a coherent quantum conductor depend on its biasing circuit. This is true even when the size of the circuit exceeds the electron coherence length, suppressing electronic interference effects. This non-intrinsic behavior can be traced to the quantum-probabilistic character of the transmission of electrons through the conductor, resulting in broad-band fluctuations of the current called shot noise [?]. This current noise can create collective excitations (hereafter called "photons") in the electromagnetic environment seen by the conductor. This yields a back action on the transport properties of the conductor itself [2]. This physics bears similarities with the spontaneous emission of photons by an excited atom, albeit with important differences: first, dc biased quantum conductors are out of equilibrium open systems and cannot be described as a set of discrete levels. Second, the dimensionless parameter characterizing the electron-photon coupling is given by the ratio of the environment's impedance to the resistance quantum $R_{\mathrm{K}} = h/e^2 \simeq 25.8\mathrm{k}\Omega$; Hence, by increasing the impedance of the circuit connected to the quantum conductor, one can significantly increase the effective coupling constant. This results in a rich physics, already partially understood: noticeably, the dynamical Coulomb Blockade (DCB) theory [2] accounts for the observed suppression [3–5] of the low voltage conductance of a tunnel element as a result of its coupling to a dissipative electromagnetic environment. A natural step is then to understand how the coupling to the environment modifies the current fluctuations themselves: is there a Coulomb Blockade of shot noise? This question of current fluctuations in the presence of DCB was addressed theoretically for the low frequency/long time limit, where the corrections to the noise power and to the full counting statistics were predicted [6–9]. Instead, we consider here the environment feedback on the frequency dependence of the shot noise of a simple quantum conductor, a tunnel junction. Following Ref. [10], we extend the DCB theory to predict the finite frequency emission noise spec-

trum of a voltage biased tunnel junction in the presence of an arbitrary linear environment. Probing this prediction requires to achieve strong coupling of the junction to its environment and to measure its high frequency shot noise. To do so, we fabricate a tunnel junction embedded in the simplest environment, a harmonic oscillator, and measure the effect of Coulomb blockade on the shot noise power at the frequency of the oscillator. The oscillator is realized with a microwave resonator based on a Josephson transmission line allowing both a tenfold increase of the coupling constant between the junction and the resonator, and to tune the resonant frequency. The data are found in quantitative agreement with the theory.

In order to evaluate the current and its fluctuations through a tunnel element in the presence of DCB, we consider a circuit consisting of a tunnel junction of conductance G_{T} in series with an impedance $Z(\nu)$ described as the series combination of harmonic modes (see upper panel of Fig. 1) at temperature T and biased at voltage V. We then compute (see the Supplemental Material for more details) the current I and the quantum spectral density $S_{\mathrm{I}}(\nu)$ of current noise, i.e. the Fourier transform of the non-symmetrized current-current correlator

$$S_{\mathrm{I}}(\nu) = 2\int_{-\infty}^{\infty}\langle I(t)I(0)\rangle e^{-i2\pi\nu t}dt. \qquad (1)$$

In this convention positive (resp. negative) frequencies correspond to energy being emitted (resp. absorbed) by the quasiparticles to (resp. from) the electromagnetic modes. Taking separate thermal equilibrium averages over the unperturbed quasiparticle and environmental degrees of freedom yields

$$I(V) = \frac{G_{\mathrm{T}}}{e}[\gamma * P(eV) - \gamma * P(-eV)],$$
$$S_{\mathrm{I}}(\nu, V) = 2G_{\mathrm{T}}[\gamma * P(eV - h\nu) + \gamma * P(-h\nu - eV)],$$

where $\gamma * P(E) = \int d\varepsilon' \gamma(\varepsilon') P(E - \epsilon')$ with $P(\varepsilon)$ the probability density for a tunneling electron to emit the energy ε in form of photons into the impedance [2], with $\gamma(\epsilon) = \int d\varepsilon' f(\varepsilon')[1 - f(\varepsilon' + \varepsilon)] = \varepsilon/(1 - e^{-\varepsilon/k_B T})$, and with f the Fermi function. Eq. 2 is the standard DCB

expression for the tunneling current [2], whereas Eq. 3 is our prediction for the Coulomb Blockade of shot noise, which we probe in the experiment described below. For a positive bias voltage and low temperature ($k_B T \ll eV, h\nu$), Eqs. 2-3 take the simpler form

$$I(V) = \frac{G_T}{e} \int_0^{eV} (eV - \varepsilon)P(\varepsilon)d\varepsilon, \qquad (2)$$

$$S_I(\nu, V) = 2G_T \Theta(eV - h\nu) \int_0^{eV - h\nu} (eV - h\nu - \varepsilon)P(\varepsilon)d\varepsilon \quad (3)$$

with $\Theta(\varepsilon)$ the Heavyside function. Eqs. 4-5 are easily interpreted: the total current is proportional to the average energy available for quasiparticles upon the transfer of an electron through the circuit, and so is the noise power at frequency ν, albeit imposing the emission of a photon of energy $h\nu$ into the environment. In the case of a vanishing impedance $Z(\nu) \ll R_K$, $P(\varepsilon) = \delta(\varepsilon)$ and one recovers the standard, non interacting, finite frequency shot noise result [11]. In the case of a discrete harmonic oscillator of frequency $\nu_0 = 1/\left[2\pi\sqrt{LC}\right]$ and impedance $Z_C = \sqrt{L/C}$, thermalized at a temperature $T \ll h\nu_0/k_B$: $P(E) = \sum_{k=0}^{\infty} p_k \delta(E - kh\nu_0)$, with $p_k = e^{-\alpha}\alpha^k/k!$ the probability for the oscillator to absorb k photons [2], and $\alpha = \pi Z_C/R_K$ the coupling strength between the tunnel junction and the oscillator. Our experiment achieves an unprecedented electron-single mode coupling $\alpha \sim 0.3$, which allows observing multi-photon processes both in the average current and in the emission noise. Note that, despite similar denominations, the effect we consider here differs from *static* Coulomb Blockade, which results from the charging energy of a small island connected to reservoirs by tunnel barrier. Static Coulomb Blockade is a quasiclassical effect which can be described by master rate equations, at the level of the current noise [12], and even the full counting statitsics [13].

Our experimental set-up is schematized in the lower panel of Fig. 1: a 100×100 nm^2 tunnel junction with tunnel resistance G_T^{-1} in the 100 kΩ range is embedded in an on-chip $\lambda/4$ coplanar resonator of resonant frequencyν_0, whose inner conductor is made of an array of identical and equally spaced Al/AlOx/Al SQUIDs. To a very good approximation, its lineic inductance is dominated by the Josephson inductance $L_J = \hbar(2eI_0|\cos(e\phi/\hbar)|a)^{-1}$, where I_0 is the maximum critical current of one SQUID, ϕ the flux applied to each SQUID, and a the distance between adjacent SQUIDs. This increases the resonator impedance Z_C above 1 kΩ, and allows to decrease ν_0 while increasing Z_C by applying a flux through the SQUIDs. Two samples were fabricated and measured. In both cases the 6 GHz maximum frequency of the resonator ensures $k_B T \ll h\nu_0$ at the 15 mK temperature of the experiment, so that thermal fluctuations do not blur Coulomb Blockade effects. The minimum zero flux lineic inductances of the first
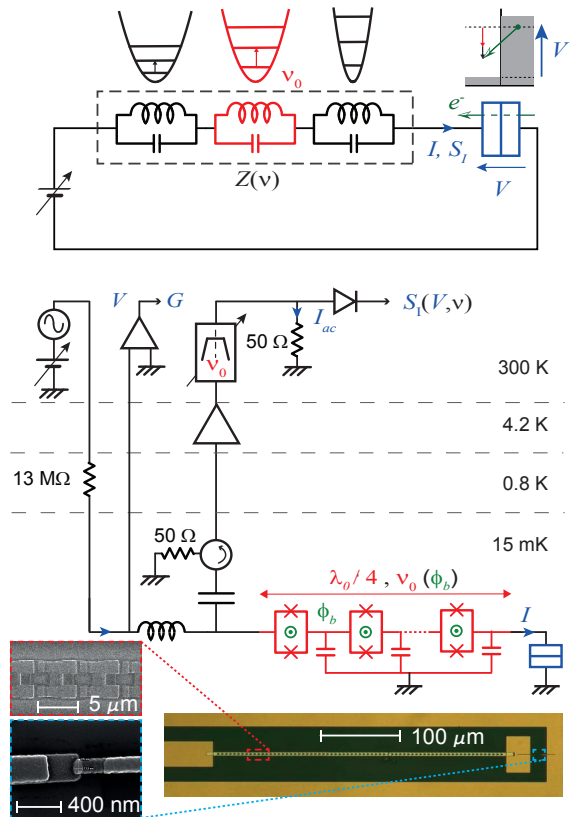

Figure 1. Coulomb Blockade in a normal quantum conductor: (a) A quantum conductor (here a tunnel junction) is voltage biased (V) through a series impedance Z modeled as a collection of harmonic modes, resulting in inelastic electron tunneling. (b) Experimental set-up: a tunnel junction is dc biased at voltage V, and connected to a SQUID-based resonator presenting a discrete mode at frequency ν_0, tuned by varying the magnetic flux ϕ_b threading each SQUID loop. The dc biasing line and 50Ω microwave measurement line are separated by a bias tee, allowing to measure the junction dc differential conductance $G(V)$ and the emission noise $S_I(\nu_0, V)$. The measurement line includes an isolator, a cryogenic amplifier with 42 dB gain, a 180 MHz passband filter centered on ν_0, and a matched quadratic detector. Temperatures of the different stages are indicated on the right. Bottom illustrations: global view of the sample, with SEM pictures of SQUIDs (top inset) forming the array and of the normal tunnel junction (bottom inset), both from sample 1

and second resonators were designed at $8.80 \ 10^{-5}$ Hm^{-1} and $3.95 \ 10^{-4}$ Hm^{-1}, respectively. Note that Josephson transmission lines have been used to create non-linear resonators used as parametric amplifiers [15], or to probe how quantum phase slips drive them into an insulating state at $Z_C \gg R_K$ [16]. We avoid this regime by keeping Z_C in the kΩ range, which stills allows us to obtain sizeable DCB corrections. Keeping the current going through the resonator much smaller than I_0 ensures that the Josephson junctions can be considered as linear inductances. The resistance G_T^{-1} being much higher than
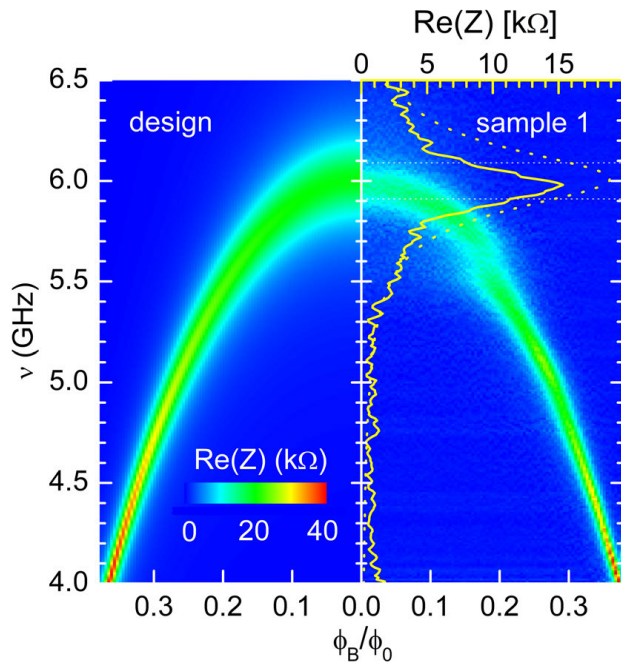
Figure 2. Characterization of the environment impedance: Designed (left) and measured (right) real part of the impedance $Z(\nu)$ of the quarter-wave resonator of sample 1 (see Fig.1) as a function of magnetic flux ϕ_b and frequency ν. The overprinted curve on the right (top scale) shows the resonance at $\nu_0 \simeq 6\text{GHz}$ for $\phi_b = 0$, measured (solid line) and calculated (dotted line). Horizontal dotted white lines indicate -3dB bandwidth used for measuring the shot noise power shown in Fig 3a.

$Z(\nu)$, the impedance seen by one conduction channel of the junction is not shunted by the parallel conductance of the other channels [17]. The SQUIDs and the tunnel junction were fabricated on a Si/SiO_2 substrate using standard nanofabrication techniques [14]. In addition, a $30 \times 50 \times 0.3 \ \mu\text{m}^3$ gold patch is inserted between the tunnel junction and the SQUID array in order to evacuate the Joule power dissipated at the tunnel junction via electron-phonon coupling. As an example, assuming a typical 2nW $\mu\text{m}^{-3}\text{K}^{-5}$ electron-phonon coupling constant [19], a $100\mu\text{V}$ (resp. 1mV) bias on a $200\text{k}\Omega$ tunnel resistance increases the electron temperature from 15mK to 20mK (resp 50mK), keeping heating effects negligible. Note that the thermalization pad adds an additional 12fF to ground, which is taken into account to evaluate the total impedance seen by the tunnel junction. The chip is connected to the biasing and measurement circuits through a commercial $50 \ \Omega$ matched bias tee. The inductive (low frequency) path is used both to bias the sample through a cold $13 \ \text{M}\Omega$ resistor, and to measure the dc voltage across the tunnel junction and its conductance $G(V)$. The capacitive (RF) path guides the radiation $S_I(\nu, V)$ emitted by the sample to a cryogenic isolator anchored at 15 mK, to a cryogenic amplifier with

a $\sim$2.5 K noise temperature in the 4-8 GHz bandwidth, to room temperature band-pass filters, and finally to a power "square law" detector, the output voltage of which is proportional to its input microwave power. The isolator diverts the current noise of the amplifier to a 50Ω matched resistor that re-emits to the sample a blackbody radiation only at the coldest temperature, ensuring a negligible photon occupation of the resonator at GHz frequencies. Finally, the signal $S_I(\nu, V)$ is extracted from the large noise floor of the cryogenic amplifier by a lock-in detection involving a 1 μV sinusoidal modulation at 17 Hz on top of the dc voltage V.

We first characterized the on-chip microwave resonator by measuring the power emitted by the electronic shot noise of the junction $S_\text{I} \sim 2eI$ at high bias voltage $V \sim$ 1 mV [20], where DCB effects are negligible. Under these conditions, the spectral density of the emitted power is $2eV\text{Re}[Z(\nu)]G_\text{T}/|1 + G_\text{T}Z(\nu)|^2 \simeq 2eVG_\text{T}\text{Re}[Z(\nu)]$ since the tunnel resistance ($G_\text{T}^{-1} =$230 kΩ /450 kΩ for sample 1/2) is much larger than the maximum detection impedance $Z(\nu)$. This spectral density is obtained using a heterodyne measurement implementing a 10 MHz-wide band pass filter at tunable frequency. As shown in Fig.2, the extracted $\text{Re}[Z(\nu)]$ is in satisfactory agreement with predictions. In particular, $Z(\nu)$ shows the expected resonance, with a resonant frequency ν_0 decreasing with ϕ, associated to an increasing impedance and quality factor, which is limited by radiative losses. The maximum disagreement between the measured maximum for $\text{Re}[Z(\nu)]$ and the calculated one is about 15%, which we attribute to an uncertainty in the calibration of the gain of the amplifying chain [14]. We attribute the additional structure around 5.7 GHz to a parasitic resonance in the detection chain. Once our microwave environment calibrated, we measure both the differential conductance $G(V)$ of the tunnel junction and the voltage derivative $\partial S_I(\nu_0, V)/\partial V$ of the noise emitted in a 180 MHz bandwidth centered around the resonator frequency ν_0, as a function of the dc bias voltage applied to the junction. The conductance, shown in the upper panel of Fig. 3 for both samples, is non-linear, showing a stair-case behavior characteristic of DCB corrections due to a single mode, rounded by the finite temperature [2]. The high characteristic impedance of our resonators yields DCB corrections to the conductance 10 times higher than with standard microwave resonators [20, 21], and shows not only the single photon emission onset at bias voltage $V_0 = h\nu_0/e$ but also the two photon onset at $2V_0$. As shown in the lower panels of Fig. 3, the voltage derivative of emission noise power also displays a non-linear staircase shape, with a first singularity at V_0, followed by a smaller step at $2V_0$. The first step at V_0 is predicted in the standard -non including DCB effects- finite frequency shot noise theory, represented by the dotted black curve in the lower panel of Fig. 3. It has been observed in several experiments [22–25] and can be dually understood either in
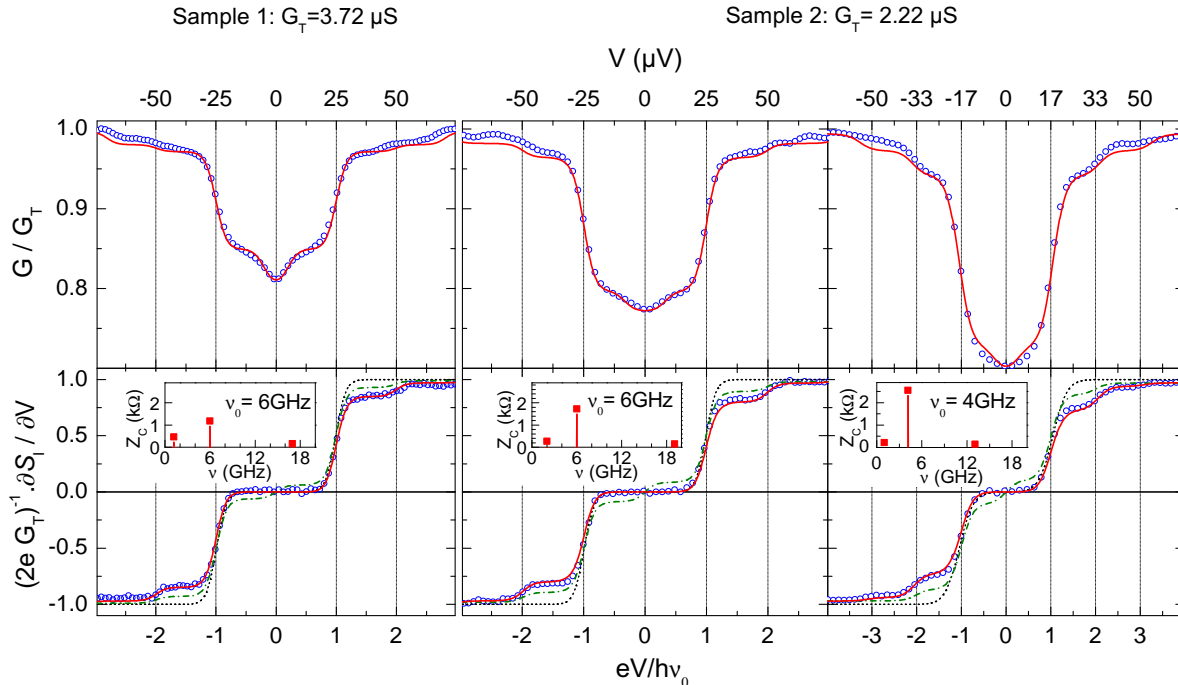
Figure 3. Comparison between the measured conductance and noise blockade, and an extension of the dynamical Coulomb blockade theory. Normalized differential conductance $G(V)$ (top) and current noise spectral density $\partial S_I(\nu_0, V)/\partial V$ (bottom). Open circles are experimental data measured at 15 mK. The left panel shows data measured on sample 1, with $\nu_0 = 6\,\text{GHz}$, the center and right panel data measured on sample 2 with $\nu_0 = 6\,\text{GHz}$ and 4 GHz, respectively. Solid red lines result from an analytical fit to the data involving series impedance made of three discrete modes shown in insets and the dotted black curve shows the non-interacting, finite frequency shot noise prediction. The green dot-dashed line represents the DCB expression for the current noise density symetrized with respect to frequency.

terms of the finite time coherence of a DC biased quantum conductor, or in terms of the energy cost of creating excitations at frequency ν_0 in the measuring apparatus [11, 26, 27]. The second step occurs at the onset voltage for the emission of two photons in the resonator by a tunneling electron. The significant difference between the experimental points and the non interacting prediction demonstrates the Coulomb Blockade of shot noise.

We now probe how the data shown in Fig. 3 can be quantitatively accounted for by Eqs. 2 and 3, using our well controlled environment as an input to evaluate $P(E)$. We model this environment as a series combination of three discrete harmonic modes. The two higher frequency ones correspond to the fundamental and first harmonic modes of the resonator. These two modes account with no adjustable parameters for the observed variations above $V_0 = h\nu_0/e$. Their characteristic impedance can be evaluated through the standard formula $Z_C = \frac{2}{\nu_0 \text{Im} Y'(\nu_0)}$, where $Y(\nu)$ is the environment's admittance, evaluated from our modeling of

the Josephson transmission line. We introduce an additional lower frequency mode to account for the unexpected 3% dip in the differential conductance that we observe at low bias voltage $|V| \lesssim 5\mu V$. We attribute this low-frequency parasitic resonance, which only slightly affects the data, to the bias-Tee. The corresponding predictions, assuming an electron temperature $T_e = 16$ mK corresponding to the temperature of the fridge's mixing chamber, are represented by the solid red curve in the top graphs of Fig. 3. Note that at this temperature, the $\sim 3.5 k_B T/h \sim 1\,\text{GHz}$ smearing expected from the Fermi distribution is broader than the linewidth of the modes of our resonator. This is why the discrete modes model, which yields analytical expression for the $P(E)$ function [2], is able to reproduce the data. The emission noise data can be reproduced by Eq. 2 with excellent accuracy, whereas the expression corresponding to the current noise spectral density symetrized with respect to frequency [10], $S_I^{\text{sym}}(\nu, V) = [S_I(-\nu, V) + S_I(\nu, V)]/2$, represented by the green dashed-dotted line in Fig.3, is not compatible with our data[14]. Note that at low tem-

perature $k_\mathrm{B}T \ll h\nu_0$ the relative size of the two-photon step is $\alpha/2$, which explains why noise blockade is not seen with usual environment impedance yielding values of $\alpha \sim 10^{-3}$. However, when considering the proposed primary shot noise thermometry [28], even such low values of α cause a systematic correction that should be considered to reach metrological accuracy. Last, the data shown in the to left panels of Fig. 3 were taken for the maximum value of $\nu_0= 6$ GHz. Applying a flux through the SQUIDs induces a stronger blockade due to the increased Josephson inductance. As shown on the right panel of Fig. 3, the higher impedance of sample 2 allows observing even three-photon processes when the resonant frequency is set at 4 GHz (the lower end of our detection bandwidth), yielding $Z_C \simeq 2.25$ kΩ and a 30% reduction of the zero-bias conductance.

---

* Presently at NEST, Istituto Nanoscienze-CNR and Scuola Normale Superiore, I-56127 Pisa, Italy

† fabien.portier@cea.fr

[1] Blanter2000 Y. Blanter and M. Büttiker, Shot noise in mesoscopic conductors," *Physics Reports*, vol. 336, no. 1–2, pp. 1 – 166, 2000.

[2] G.-L. Ingold and Y. V. Nazarov, "Charge tunneling rates in ultrasmall junctions," in *Single Charge Tunneling* (H. Graber and M. H. Devoret, eds.), Plenum Press (New York and London), 1992.

[3] A. N. Cleland, J. M. Schmidt, and J. Clarke, "Influence of the environment on the coulomb blockade in submicrometer normal-metal tunnel junctions," *Phys. Rev. B*, vol. 45, pp. 2950–2961, Feb 1992.

[4] P. Delsing, K. K. Likharev, L. S. Kuzmin, and T. Claeson, "Effect of high-frequency electrodynamic environment on the single-electron tunneling in ultrasmall junctions," *Phys. Rev. Lett.*, vol. 63, pp. 1180–1183, Sep 1989.

[5] L. J. Geerligs, V. F. Anderegg, C. A. van der Jeugd, J. Romijn, and J. E. Mooij, "Influence of dissipation on the coulomb blockade in small tunnel junctions," *EPL (Europhysics Letters)*, vol. 10, no. 1, p. 79, 1989.

[6] A. V. Galaktionov, D. S. Golubev, and A. D. Zaikin, "Current fluctuations and electron-electron interactions in coherent conductors," *Phys. Rev. B*, vol. 68, p. 85317, Aug 2003.

[7] M. Kindermann and Y. V. Nazarov, "Interaction effects on counting statistics and the transmission distribution," *Phys. Rev. Lett.*, vol. 91, p. 136802, Sep 2003.

[8] M. Kindermann, Y. V. Nazarov, and C. W. J. Beenakker, "Feedback of the electromagnetic environment on current and voltage fluctuations out of equilibrium," *Phys. Rev. B*, vol. 69, p. 35336, Jan 2004.

[9] I. Safi and H. Saleur, "One-channel conductor in an ohmic environment: Mapping to a tomonaga-luttinger liquid and full counting statistics," *Phys. Rev. Lett.*, vol. 93, p. 126602, Sep 2004.

[10] H. Lee and L. S. Levitov, "Current fluctuations in a single tunnel junction," *Phys. Rev. B*, vol. 53, pp. 7383–7391, Mar 1996.

[11] G.B. Lesovik and R. Loosen, "On the detection of the finite frequency current fluctuations," *JETP Lett.* vol. 65, p. 295 (1997). Here the distinction is made between emission noise $S_\mathrm{I}(\nu) = 2 \int_{-\infty}^{\infty} \langle I(t)I(0)\rangle e^{-i2\pi\nu t}dt$ and absorbtion noise $S_\mathrm{I}(-\nu)$. While observation of the later requires excitation of the sample by external sources, for a zero temperature external circuit, only $S_\mathrm{I}(\nu)$ is observed. For an earlier high-frequency shot noise derivation not making the distinction between $S_\mathrm{I}(\nu)$ and $S_\mathrm{I}(-\nu)$, see V.A. Khlus, *Zh. Eksp. Teor. Fiz.*, vol. 93, p. 2179 (1987) [*Sov. Phys. JETP*, vol. 66, p. 1243 (1987)] and G.B. Lesovik, *Prisma Zh. Eksp. Teor. Fiz.* vol. 49, p. 513 (1989) [*JETP Lett.* vol. 66, p. 592 (1989)].

[12] S. Kafanov and P. Delsing, "Measurement of the shot noise in a single-electron transistor," *Phys. Rev. B*, vol. 80, p. 155320, Oct 2009.

[13] S. Gustavsson, R. Leturcq, B. Simovi, R. Schleser, P. Studerus, T. Ihn, K. Ensslin, D. C. Driscoll and A. C. Gossard, "Counting statistics and super-Poissonian noise in a quantum dot: Time-resolved measurements of electron transport," *Phys. Rev. B*, vol. 74, p. 195305, Nov 2006.

[14] For more information, see the Supplementary Material.

[15] M. A. Castellanos-Beltran, K. D. Irwin, G. C. Hilton, L. R. Vale, and K.W. Lehnert, "Amplification and squeezing of quantum noise with a tunable Josephson metamaterial," *Nature Physics*, vol. 4, pp. 229-231, Dec 2008.

[16] E. Chow, P. Delsing, and D. B. Haviland, "Length-Scale Dependence of the Superconductor-to-Insulator Quantum Phase Transition in One Dimension," *Phys. Rev. Lett.*, vol. 81, pp. 204–207, Jul 1998.

[17] P. Joyez, D. Esteve and M. H. Devoret, "How Is the Coulomb Blockade Suppressed in High-Conductance

Tunnel Junctions?," *Phys. Rev. Lett.*, vol. 80, pp. 1956–1959, Mar 1998.

[18] I. M. Pop, T. Fournier, T. Crozes, F. Lecocq, I. Matei, B. Pannetier, O. Buisson, and W. Guichard, "Fabrication of stable and reproducible submicron tunnel junctions," J. Vac. Sci. Technol. B vol. 30, p 010607, Jan 2012.

[19] B. Huard, H. Pothier, D. Esteve and K. E. Nagaev, "Electron heating in metallic resistors at sub-Kelvin temperature," *Phys. Rev. B*, vol. 76, p. 165426, Oct 2007.

[20] M. Hofheinz, F. Portier, Q. Baudouin, P. Joyez, D. Vion, P. Bertet, P. Roche, and D. Esteve,"The Bright Side of Coulomb Blockade," *Phys. Rev. Lett.*, vol. 106, p. 217005, May 2011.

[21] T. Holst, D. Esteve, C. Urbina, and M.H. Devoret, "Effect of a transmission line resonator on a small capacitance tunnel junction," *Phys. Rev. Lett.*, vol. 73, pp. 3455–3458, Dec 1994.

[22] R.J. Schoelkopf, P. J. Burke, A.A. Kozhevnikov, D.E. Prober, and M.J. Rooks, "Frequency dependence of shot noise in a diffusive mesoscopic conductor," *Phys. Rev. Lett.*, vol. 78, pp. 3370–3373, Apr 1997.

[23] E. Onac, F. Balestro, L.H.W. van Beveren, U. Hartmann, Y.V. Nazarov, and L.P. Kouwenhoven, "Using a quantum dot as a high-frequency shot noise detector," *Phys. Rev. Lett.*, vol. 96, p. 176601, May 2006.

[24] E. Zakka-Bajjani, J. Ségala, F. Portier, P. Roche, D. C. Glattli, A. Cavanna, and Y. Jin, "Experimental test of the high-frequency quantum shot noise theory in a quantum point contact," *Phys. Rev. Lett.*, vol. 99, p. 236803, Dec 2007.

[25] S. Gustavsson, M. Studer, R. Leturcq, T. Ihn, K. Ensslin, D. C. Driscoll, and A. C. Gossard, "Frequency-selective single-photon detection using a double quantum dot," *Phys. Rev. Lett.*, vol. 99, p. 206804, Nov 2007.

[26] U. Gavish, Y. Levinson, and Y. Imry, "Detection of quantum noise," *Phys. Rev. B*, vol. 62, p. R10637, Oct 2000.

[27] R. Aguado and L. P. Kouwenhoven, "Double quantum dots as detectors of high-frequency quantum noise in mesoscopic conductors," *Phys. Rev. Lett.*, vol. 84, pp. 1986–1989, Feb 2000.

[28] L. Spietz, K.W. Lehnert, I. Siddiqi and R.J. Schoelkopf, "Primary Electronic Thermometry Using the Shot Noise of a Tunnel Junction," *Science*, vol. 300, pp. 1929-1932 , June 2003.

[29] D. S. Golubev and A. D. Zaikin, "Coulomb interaction and quantum transport through a coherent scatterer," *Phys. Rev. Lett.*, vol. 86, pp. 4887–4890, May 2001.

[30] A. Levy Yeyati, A. Martin-Rodero, D. Esteve, and C. Urbina, "Direct link between coulomb blockade and shot noise in a quantum-coherent structure," *Phys. Rev. Lett.*, vol. 87, p. 46802, Jul 2001.

[31] R. Cron *et al.* in *Electronic Correlations: From Meso to Nano-Physics* (T. Martin, G. Montambaux, and J. T. T. Vân, eds.), EDP Sciences, Les Ulis, 2001.

[32] C. Altimiras, U. Gennser, A. Cavanna, D. Mailly, and F. Pierre, "Experimental test of the dynamical coulomb blockade theory for short coherent conductors," *Phys. Rev. Lett.*, vol. 99, p. 256805, Dec 2007.

[33] J. R. Souquet, I. Safi and P. Simon, "Dynamical Coulomb blockade in an interacting one-dimensional system coupled to an arbitrary environment," *Phys. Rev. B*, vol. 88, p. 205419, Nov 2013.

[34] F. D. Parmentier, A. Anthore, S. Jezouin, H. le Sueur, U. Gennser, A. Cavanna, D. Mailly, and F. Pierre, "Strong back-action of a linear circuit on a single electronic quantum channel," *Nature Physics*, vol. 7, pp. 935–938, Dec. 2011.

[35] S. Jezouin, M. Albert, F. D. Parmentier, A. Anthore, U. Gennser, A. Cavanna, I. Safi, and F. Pierre, "Tomonaga–Luttinger physics in electronic quantum circuits," *Nature Communications*, vol. 4, p. 1802, apr 2013.

[36] H. T. Mebrahtu *et al.*, "Quantum phase transition in a resonant level coupled to interacting leads," *Nature*, vol. 488, pp. 61–64, Apr 2012.

Supplemental Material for the article "Dynamical Coulomb Blockade of Shot Noise"

Carles Altimiras,* Olivier Parlavecchio, Philippe Joyez, Denis Vion, Patrice Roche, Daniel Esteve, and Fabien Portier

Service de Physique de l'Etat Condensé (CNRS URA 2464),
IRAMIS, CEA-Saclay, 91191 Gif-sur-Yvette, France
(Dated: September 20, 2013)

CALCULATION OF THE CURRENT NOISE

The circuit we consider consists of a pure tunnel element connected in series with an arbitrary linear electromagnetic environment (See Fig. 1 of the main text). In this picture, the capacitance of the real tunnel junction has been incorporated into the impedance of the electromagnetic environment [1]. The Hamiltonian of the circuit is:

$$H = H_0 + H_{\rm T}.$$

with

$$H_0 = \sum_\ell \varepsilon_\ell c_\ell^\dagger c_\ell + \sum_r \varepsilon_r c_r^\dagger c_r + H_{\rm env}.$$

Here, the indexes ℓ and r span all quasiparticle states in the left and right electrodes, the $c_{\ell,r}^\dagger$ (resp. $c_{\ell,r}$) denote the fermionic quasiparticle creation (resp. destruction) operators, $H_{\rm env}$ is the Hamiltonian of the electromagnetic environment, and $H_{\rm T} = T + T^\dagger$ is the tunneling Hamiltonian with T and $T^\dagger$ implementing the transfer of one electron across the barrier from left to right and from right to left, respectiveley. This operator can be decomposed as $T = e^{i\varphi}\Theta$ where the $e^{i\varphi}$ operator acts only on the electromagnetic environment by translating the charge transfered through the impedance by e, the charge of the tunneling electron, while $\Theta = \sum_{\ell,r} \tau_{\ell r} c_\ell^\dagger c_r$ acts only on the quasiparticles in the electrodes. In this writing $\tau_{\ell r}$ is the tunnel coupling amplitude of states ℓ and r, and φ denotes the phase difference operator across the tunnel element, acting on the electromagnetic environment, and related to the voltage drop V across the tunnel element by $V = \frac{\hbar}{e}\frac{\partial \varphi}{\partial t}$. The current operator through the tunnel element is given by $I = -\frac{e}{\hbar}\frac{\partial H}{\partial \varphi} = -i\frac{e}{\hbar}(T - T^\dagger)$.

The non-symmetrized noise current density $S_{\rm I}(\nu)$ is the Fourier transform of the current-current correlator:

$$S_{\rm I}(\nu) = 2 \int_{-\infty}^{\infty} \langle I(t)I(0)\rangle e^{-i2\pi\nu t} dt \qquad (1)$$

In this convention positive (resp. negative) frequencies correspond to energy being emitted (resp. absorbed) by the quasiparticles to (resp. from) the electromagnetic modes, and the current-current correlator function reads

$$\langle I(t)I(0)\rangle = \frac{e^2}{\hbar^2}\{\langle T(t)T^\dagger(0)\rangle + \langle T^\dagger(t)T(0)\rangle\}.$$

We evaluate the averages by taking separate thermal equilibrium averages over the unperturbed quasiparticles and environmental degrees of freedom:

$$\langle I(t)I(0)\rangle = \frac{e^2}{\hbar^2}\left\{ \langle e^{i\varphi(t)}e^{-i\varphi(0)}\rangle\langle\Theta(t)\Theta^\dagger(0)\rangle \right. \qquad (2)$$
$$\left. + \langle e^{-i\varphi(t)}e^{i\varphi(0)}\rangle\langle\Theta^\dagger(t)\Theta(0)\rangle \right\}.$$

Unless at zero bias voltage where Eq. 2 is always exact, this amounts to assuming that there exist unspecified relaxation mechanisms fast enough to restore thermal equilibrium both in the electrodes and in the impedance between tunneling events. The validity of this latter assumption is highly dependent on the details of the system and should be checked on a case by case basis.

Within this assumption, the occupation probability of the quasiparticle energy levels in the electrodes is given by the Fermi function $f(\epsilon)$ at the inverse temperature β. We further assume constant densities of states ρ_l, ρ_r in the electrodes and we replace the $|\tau_{\ell r}|^2$ by their average value $|\tau|^2$ over all l,r states. The average over quasiparticles degrees of freedom thus takes the form

$$\langle\Theta(t)\Theta^\dagger(0)\rangle = \left\langle \sum_{\ell,r} |\tau_{\ell r}|^2 c_\ell^\dagger(t)c_\ell(0)c_r(t)c_r^\dagger(0) \right\rangle$$

$$= |\tau|^2 \rho_l \rho_r \int d\varepsilon d\varepsilon' f(\varepsilon)(1 - f(\varepsilon + \varepsilon'))e^{-i\varepsilon' t/\hbar}$$

$$= \frac{\hbar G_T}{2\pi e^2} \int d\varepsilon' \gamma(\varepsilon')e^{-i\varepsilon' t/\hbar}$$

$$= \frac{\hbar G_T}{2\pi e^2} \tilde{\gamma}(t),$$

where $G_T = 4\pi^2 G_K |\tau|^2 \rho_l \rho_r$ denotes the tunnel conductance of the junction, which we assume much smaller than $G_K = e^2/h$, allowing to treat H_T at the lowest order in perturbation theory; $\tilde{\gamma}(t)$ denotes the inverse Fourier transform of

$$\begin{aligned} \gamma(\epsilon) &= \int d\varepsilon' f(\varepsilon')(1 - f(\varepsilon' + \varepsilon)) \\ &= \frac{\epsilon}{1 - e^{-\beta\epsilon}} \\ &= \frac{\epsilon}{2}\left(1 + \coth\frac{\beta\epsilon}{2}\right) \\ &= n_B(|\epsilon|) + \epsilon\,\theta(\epsilon), \end{aligned}$$

where n_B is the Bose distribution function. The function $\gamma(\epsilon)$ is proportional to the number of possible electron-hole excitations in the Fermi seas of the electrodes with an energy difference of ϵ between the final and initial states. The same function is encountered in other contexts, such as in the noise of a resistor, for emission and

absorption by bosonic degrees of freedom (see below). Even though $\gamma(\epsilon)$ is not bounded, its inverse Fourier transform can nevertheless be expressed using distribution functions, meant to be integrated with proper functions [2, 3]:

$$\tilde{\gamma}(t) = i\pi\hbar^2 \frac{d}{dt}\delta(t) - \frac{\pi^2}{\beta^2}\sinh^{-2}\frac{\pi t}{\hbar\beta}. \qquad (3)$$

The second quasiparticle term $\langle\Theta^\dagger(t)\Theta(0)\rangle$ can be checked to give the same result, i.e. $\langle\Theta^\dagger(t)\Theta(0)\rangle = \langle\Theta(t)\Theta^\dagger(0)\rangle$.

To evaluate the average over the electromagnetic degrees of freedom, we decompose the phase difference across the tunnel element $\varphi(t) = \varphi_0(t) + \tilde{\varphi}(t)$ into the deterministic part $\varphi_0(t) = eVt/\hbar$ corresponding to the dc voltage V across the junction, and a fluctuating random phase $\tilde{\varphi}(t)$ caused by the fluctuations in the electromagnetic environment. For a linear electromagnetic environment at equilibrium, phase fluctuations are Gaussian. In this case, the averages we need to evaluate in Supplemental Material Eq. 2 can be expressed as $\langle\exp\pm i\tilde{\varphi}(t)\exp\mp i\tilde{\varphi}(0)\rangle = \exp J(t)$, where $J(t) = \langle(\tilde{\varphi}(t) - \tilde{\varphi}(0))\tilde{\varphi}(0)\rangle$ is the phase-phase correlation function [1]. The phase being proportional to the time derivative of the voltage, the phase-phase correlation function is related to the voltage noise on impedance seen by the junction, which can be obtained by the quantum fluctuation-dissipation theorem [1]:

$$J(t) = hR_K^{-1}\int_{-\infty}^{+\infty}\frac{S_V(\nu)}{(h\nu)^2}(e^{-i2\pi\nu t} - 1)d\nu, \qquad (4)$$

with

$$S_V(\nu) = 2\mathrm{Re}Z(\nu)\gamma(h\nu)$$

being the (equilibrium) non-symmetrized voltage noise across the environment impedance [4]. Collecting the above terms in Supplemental Material Eq. 2, we obtain the final expression for the current-current correlator:

$$\langle I(t)I(0)\rangle = \frac{G_T}{2\pi\hbar}2\cos\frac{eVt}{\hbar}e^{J(t)}\tilde{\gamma}(t).$$

Inserting this result in the Fourier transform (1), the current noise can be expressed as

$$S_I(\nu) = 2G_T[\gamma * P(-h\nu + eV) + \gamma * P(-h\nu - eV)],$$

where $*$ denotes convolution, and $P(E) = \frac{1}{2\pi\hbar}\int_{-\infty}^{\infty}e^{J(t)+iEt/\hbar}dt$ is the Fourier transform of $\exp[J(t)]$. This function $P(E)$ is interpreted as the probability for the environment to absorb the algebraical energy E during a tunnel event, and the convolution product:

$$\gamma * P(E) = \int d\varepsilon'\gamma(\varepsilon')P(E - \epsilon')$$

simply accounts for all the possible ways to split an energy E between the quasiparticles degrees of freedom and the environment modes. For the case of an environment of vanishing impedance, $P(E) \to \delta(E)$, and we recover a well known result

$$S_I(\nu) \to S_I(\nu) = 2G_T[\gamma(-h\nu + eV) + \gamma(-h\nu - eV)].$$

SAMPLE FABRICATION

The 300 nm thick gold ground plane of the resonator and thermalization pad were obtained by optical lithography, followed by evaporation and lift-off. SQUIDs where fabricated following the process described in Ref. [5]: the SQUIDs (see the top inset) are obtained by double angle deposition of $(20/40\,\mathrm{nm})$ thin aluminum electrodes, with a $20'$ oxydation of the first electrode at $400\,\mathrm{mBar}$ of a $(85\%\,O_2/15\%\,Ar)$ mixture. Before the evaporation, the substrate was cleaned by rinsing in ethanol and Reactive Ion Etching in an oxygen plasma [6]. The normal junction was obtained using the same technique, with $30/60$ nm thick copper electrodes and an aluminum oxyde tunnel barrier (5 nm thick aluminum oxidized for 15 minutes at a 800 mBar $(85\%O_2, 15\%Ar)$ mixture).

DETAILS ON THE JOSEPHSON
TRANSMISSION LINE

For sample 1 (resp. 2), our resonator consists in a $360\,\mu\mathrm{m}$ (resp. $91\,\mu\mathrm{m}$) long Josephson metamaterial line containing 72 (resp. 38) lithographically identical and evenly spaced SQUIDs with a $5\,\mu\mathrm{m}$ (resp. $2.4\,\mu\mathrm{m}$) period. The SQUIDs tunnel barriers of sample 1 (resp. sample 2) have an area of $0.5\,\mu\mathrm{m}^2$ (resp. $0.5\,\mu\mathrm{m}^2$) each resulting in a room temperature tunnel resistance $R_N = 720\,\Omega$ (resp. $R_N = 1880\,\Omega$). To assess that the SQUIDs in the array are identical, we have performed reproducibility tests, yielding constant values of R_N (within a few %) over millimetric distances. Assuming a superconducting gap $\Delta = 180\,\mu\mathrm{eV}$ and a 17% increase of the tunnel resistance between room temperature and base temperature [7], one obtains a zero flux critical current for the SQUIDs $I_C = 671$nA for sample 1 and $I_C = 268$ nA, corresponding to $L_J(\phi = 0) = 0.49$ nH for sample 1 and $L_J(\phi = 0) = 1.25$ nH for sample 2. This corresponds to an effective lineic inductance $\mathcal{L} \simeq 100\,\mu\mathrm{H.m}^{-1}$ at zero magnetic flux and frequency much lower than the Josephson plasma frequency of the junctions ν_P[8]. Assuming a capacitance for the junctions of the order of 80 fF/$\mu\mathrm{m}^2$ yields $\nu_P \simeq 25$ GHz. Note that our simple fabrication mask produces 10 times bigger Josephson junction in between adjacent SQUIDs, resulting in an additional $\sim \mathcal{L} \simeq 10\,\mu\mathrm{H.m}^{-1}$ lineic inductance for sample 1 and $\sim \mathcal{L} \simeq 25\,\mu\mathrm{H.m}^{-1}$ for sample 2. The

$\sim \mathcal{L} \simeq 1\,\mu\text{H.m}^{-1}$ electromagnetic inductance associated to our geometry is negligible. With the designed lineic capacitance $\mathcal{C} = 75\,\text{pF.m}^{-1}$, the length of the resonator sets the first resonance at $\nu_0 \simeq 8\,\text{GHz}$ for sample 1 and $\nu_0 \simeq 12\,\text{GHz}$ for sample 2. The 12 fF shunting capacitance of the themalization pad reduces these frequencies to $\nu_0 \simeq 6\,\text{GHz}$ in both cases.

DETAILS ON SETUP AND CALIBRATION

We describe the calibration of the low frequency circuitry for voltage bias and current measurement as well the microwave components used to define the environment of the junction and to measure the emitted radiation.

Low frequency circuit

In addition to the components depicted in Fig. 1 of the main text, the low frequency circuit includes a copper powder filter anchored on the mixing chamber, as well as a distributed RC filter made with a resistive wire (50 cm of IsaOhm 304 Ω m^{-1}) winded around a copper rod, and glued with silver epoxy on a copper plate in good thermal contact with the mixing chamber. Both are inserted between the 13 MΩ bias resistor and the bias T and are represented by the 170Ω/450 pF RC filter on the biasing line in Supplemental Material Fig. 1. The distributed RC filter has two benefits on the effective electron temperature of our experiment: it provides a high frequency filtering that reduces the polarisation noise as well as thermalisation of the electrons. The copper powder filter is meant to absorb parasitic microwave noise. The line allowing to measure the low frequency response of the junction is filtered by a multipole RC low pass filter, made with a succession of 2 kΩ Nickel-Chromium resistances and 1 nF capacitances to ground. The NiCr resistances were checked in an independent cool-down to change by less than 1%, which allows to calibrate the 13 MΩ resitor in-situ, with a precision better than 1%, which in turn allows us to determine the dc voltage V applied to the tunnel junction. The validity of this callibrattion is confirmed by the quality of the comparison between the observed steps in $\partial S_I(\nu)/\partial V$ and our predictions.

Microwave circuit and calibration

The microwave chain comprises a bias T, two 4-8 GHz cryogenic circulators anchored at the mixing chamber, as well as a 4-8 GHz bandpass filter and a 12 GHz low pass gaussian absorptive filter (see Supplemental Material Fig. 2). These elements are anchored on the mixing chamber

and are meant to protect the sample from the back-action noise of the amplifier. The quantitative determination of the detection impedance relies on the detection of the power emitted by the shot noise of the tunnel junction in the high bias regime. We bias the junction at $\sim 1\,\text{mV}$, where DCB corrections are negligible, so that $S_I = 2eI$ at frequencies $|\nu| \ll eV/h \simeq 0.5\,\text{THz}$. In order to separate this noise from the noise floor of the cryogenic amplifier, we then apply small variations of the bias voltage and measure the corresponding changes in the measured microwave power with a lock-in amplifier. The conversion of S_I into emitted microwave power depends on the environment impedance $Z(\nu)$ seen by the tunneling resistance R_T. First, only a fraction $R_T^2/|R_T + Z(\nu)|^2$ of the current noise is absorbed by the environment. The current noise in the environment has then to be multiplied by $\text{Re}[Z(\nu)]$ to obtain the microwave power emitted by the electronic shot noise:

$$S_P(\nu) = 2eV \frac{\text{Re}[Z(\nu)]G_T^{-1}}{|Z(\nu) + G_T^{-1}|^2} \simeq 2eV \frac{\text{Re}[Z(\nu)]G_T^{-1}}{[\text{Re}[Z(\nu)] + G_T^{-1}]^2}. \tag{5}$$

The last approximation, $\text{Im}[Z(\nu)] \ll G_T^{-1}$ is satisfied with a precision better than 2%. Finally, what is actually detected at room temperature is the amplified microwave power:

$$S_P^{\text{RT}}(\nu) = 2eVG(\nu) \frac{\text{Re}[Z(\nu)]G_T^{-1}}{[\text{Re}[Z(\nu)] + G_T^{-1}]^2}. \tag{6}$$

Supplemental Material Eq. 6 shows that the extracted $\text{Re}[Z(\nu)]$ depends on the gain of the microwave chain $G(\nu)$, which has to be determined in-situ and independently. To do so, we inserted a 20 dB directional coupler between the sample and the bias Tee, and injected through an independently calibrated injection line, comprising 70 dB attenuation distributed between 4.2 K and the mixing chamber temperature (see Supplemental Material Fig. 2). Both the attenuators and the directional coupler were calibrated at 4.2 K. The resonator is tuned at a resonance well below 4 GHz, so that the entire microwave power is reflected by the sample, allowing to calibrate the gain of the detection chain, albeit doubling the insertion losses of the bias Tee and of the 10 cm microwave cable connecting it to the sample. However, this parasitic contribution can be substracted thanks to independent calibrations. Due to lack of space, we then had to remove one of the circulators for this experiment, which increased the electronic temperature from 16 mK to 25 mK, which explains that we calibrated the detection impedance in an independant run of the experiment.

EXTRACTING THE CURRENT NOISE

We discuss here the possible consequences of the fact that the detection impedance is not negligible compared

to the tunneling resistance. More specifically, we show that due to the variations of the tunneling resistance with bias voltage, measuring $\partial S_P(\nu)/\partial V$ is not rigorously equivalent to measuring $\partial S_I/\partial V$. However, the error introduced by this approximation can be shown to be negligible.

Due to the non linearity of the tunnel transfer, the power emitted by the junction biased at bias V reads

$$S_P(\nu) = \text{Re}[Z(\nu)] \left| \frac{Z_T(\nu, V)}{Z(\nu) + Z_T(\nu, V)} \right|^2 S_I(V, \nu). \quad (7)$$

Here $Z_T(\nu, V)$ is the differential impedance of the junction, biased at voltage V, at the measurement frequency ν. Supplemental Material Eq. 7 is valid as long as the ac current going through the junction as a consequence of the shot noise is small enough for the response of the junction $Z_T(\nu, V)$ to remain in the linear regime. In that case, the modulation of the output voltage of the quadractic detector that we measure is proportional to

$$\frac{\partial S_P(\nu)}{\partial V} = \text{Re}[Z(\nu)] \left[\left| \frac{Z_T(\nu, V)}{Z(\nu) + Z_T(\nu, V)} \right|^2 \frac{\partial S_I(V, \nu)}{\partial V} \right.$$
$$\left. + S_I(V, \nu) \frac{\partial}{\partial V} \left| \frac{Z_T(\nu, V)}{Z(\nu) + Z_T(\nu, V)} \right|^2 \right]. \quad (8)$$

We can deduce the expected variations of $Z_T(\nu, V)$ with bias voltage from the dc transport properties of the junction via

$$Z_T^{-1}(\nu, V) = \frac{e}{2h\nu}[I(V + h\nu/e) - I(V - h\nu/e)]. \quad (9)$$

Inserting Eq. 9 in Eq. 8 shows that the associated corrections are negligeable, so that detecting $\frac{\partial S_P(\nu)}{\partial V}$ gives direct access to $\frac{\partial S_I(V, \nu)}{\partial V}$ within a precision better than 1%.

NOTE ON NOISE SYMETRIZATION

Let us add a note about the symetrization of the correlator being measured in our high frequency noise measurements. On one hand the microwave amplifier probes its input voltage [4], which can be written as

$$V_{\text{in}}(t) = -\sqrt{\frac{\hbar Z_0}{4\pi}} \int_B \omega^{1/2}(i a_{\text{in}}(\omega) e^{-i\omega(t-x/c)} + \text{h.c.}) d\omega, \quad (10)$$

where $a_{\text{in}}(\omega)$ stands for the destruction operator of a input (right moving) photon at frequency ω, c is the velocity of electromagnetic waves in the transmission line connecting the sample to the amplifier, of characteristic impedance $Z_0 = 50\Omega$, and B the measurement bandwidth. The output voltage reads:

$$V_{\text{out}}(t) = -\sqrt{\frac{\hbar Z_0}{4\pi}} \int_B \omega^{1/2}(i a_{\text{out}}(\omega) e^{-i\omega(t-x/c)} + \text{h.c.}) d\omega, \quad (11)$$

with

$$a_{\text{out}} = \sqrt{G} a_{\text{in}} + \sqrt{G-1} f^\dagger \quad (12)$$

with G the gain of the amplifier and $f^\dagger$ representing the amplifier's noise [4]. Thus the final power measurement $\propto < V_{\text{out}}^2 >$ contains, on top of the amplifier's noise, a term proportional to

$$\langle V_{\text{in}}^2 \rangle = \frac{\hbar Z_0}{4\pi} \int_B \omega \left\langle a_{\text{in}}(\omega) a_{\text{in}}^\dagger(\omega) + a_{\text{in}}^\dagger(\omega) a_{\text{in}}(\omega) \right\rangle d\omega \quad (13)$$

$$= \frac{\hbar Z_0}{2\pi} \int_B \omega \left[\left\langle a_{\text{in}}^\dagger(\omega) a_{\text{in}}(\omega)) \right\rangle + \frac{1}{2} \right] d\omega, \quad (14)$$

thus containing a power representing the zero point motion of the line, associated to a power $\hbar\omega/2$ per unit bandwidth. In other words, the amplifier gives access to the sum of the absorption and emission noise of the input line, unlike quantum detectors [9, 10] which allow detecting them separately. However, this does not imply that we measure the *electronic current noise of the sample* symetrized with respect to frequency: In our experiment, we measure the excess output noise power associated to the dc biasing of our sample. This results in a excess population of the input field $< a_{\text{in}}^\dagger(\omega) a_{\text{in}}(\omega) >$, which is itself proportional to the photons leakage rate out of our resonator. Thanks to the circulators anchored at the mixing chamber temperature $T \ll h\nu_0/k_B$, the latter is kept very close to its ground state (the maximum average number of photons in the resonator is below 5% for the experiments reported in the paper), and can thus only absorb energy from the electronic current fluctuations (in other words $P(h\nu) \ll P(-h\nu)$). This is why our signal is proportional to the emission noise power $S_I(\nu, V)$ and not the noise power symetrized with respect to frequency $S_I^{\text{sym}}(\nu, V) = [S_I(-\nu, V) + S_I(\nu, V)]/2$, which also contains the electronic zero point motion.

---

* *Note:* Presently at NEST, Istituto Nanoscienze-CNR and Scuola Normale Superiore, I-56127 Pisa, Italy

[1] G.-L. Ingold and Y. V. Nazarov, "Charge tunneling rates in ultrasmall junctions," in *Single Charge Tunneling* (H. Graber and M. H. Devoret, eds.), Plenum Press (New York and London), 1992.

[2] P. Joyez and D. Esteve, "Single-electron tunneling at high temperature," *Phys. Rev. B*, vol. 56, pp. 1848–1853, Jul 1997.

[3] A. A. Odintsov, "Effect of dissipation on dynamic characteristics of small tunnel junctions in terms of the polaron

model," *Soviet Journal of Low Temperature Physics*, vol. 15, pp. 263–266, May 1989.

[4] See A. A. Clerk, M. H. Devoret, S. M. Girvin, F. Marquardt, and R. J. Schoelkopf, "Introduction to quantum noise, measurement, and amplification," *Rev. Mod. Phys.*, vol. 82, pp. 1155–1208, Apr 2010 and references therein.

[5] I. M. Pop, T. Fournier, T. Crozes, F. Lecocq, I. Matei, B. Pannetier, O. Buisson, and W. Guichard, "'Fabrication of stable and reproducible submicron tunnel junctions,"' J. Vac. Sci. Technol. B vol. 30, p 010607, Jan 2012.

[6] Following Ref. [5], we performed Reactive Ion Etching under an oxygen pressure of 0.3 mbar and 10W RF power, during 15 seconds, in a Plassys MG -200- S RIE equipment.

[7] K.Gloos, R. S. Poikolainen and J. P. Pekola, App. Phys. Lett. **77**,2915 (2000).

[8] B. D. Josephson, Rev. Mod. Phys **36**, 216 (1964).

[9] J. Basset, H. Bouchiat, and R. Deblock, Phys. Rev. Lett. **105**, 166801 (2010).

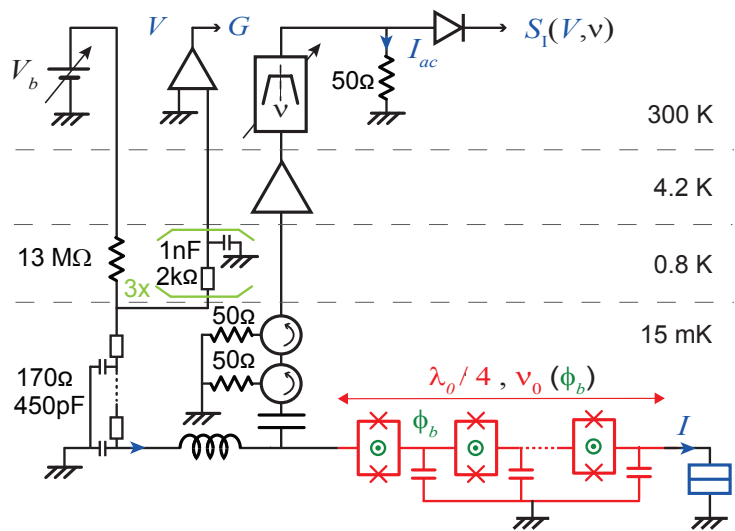[10] J. Basset, H. Bouchiat, and R. Deblock, Phys. Rev. B **85**, 085435 (2012).

Figure 1. More detailled view of the experimental setup. Only circuit components inside the refrigerator are shown in full detail.
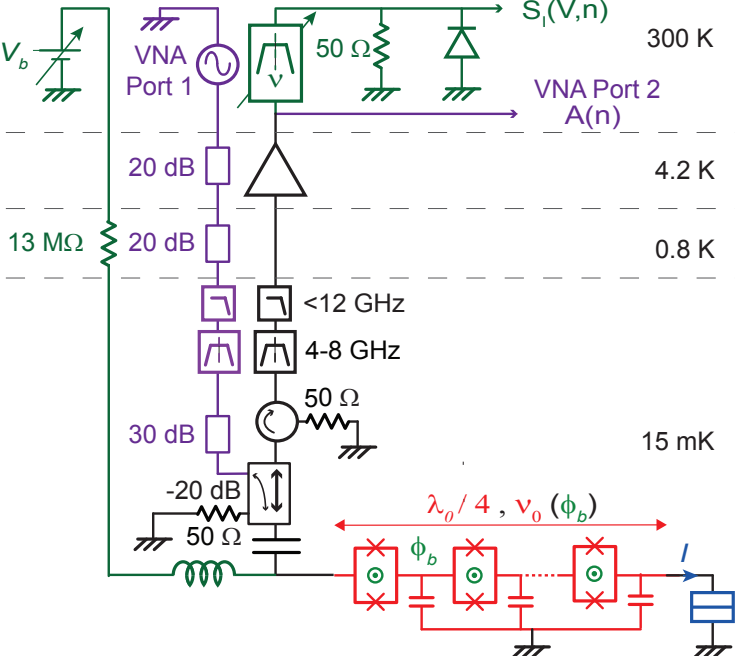

Figure 2. Characterization of the environment impedance: the microwave chain is calibrated using a vectorial network analyzer, setting the resonance frequency well below 4 GHz.